

We are IntechOpen, the world's leading publisher of Open Access books Built by scientists, for scientists

6,900

Open access books available

186,000

International authors and editors

200M

Downloads

Our authors are among the

154

Countries delivered to

TOP 1%

most cited scientists

12.2%

Contributors from top 500 universities



WEB OF SCIENCE™

Selection of our books indexed in the Book Citation Index
in Web of Science™ Core Collection (BKCI)

Interested in publishing with us?
Contact book.department@intechopen.com

Numbers displayed above are based on latest data collected.
For more information visit www.intechopen.com



Passive Q-switched and Mode-locked Fiber Lasers Using Carbon-based Saturable Absorbers

Mohd Afiq Ismail, Sulaiman Wadi Harun, Harith Ahmad and
Mukul Chandra Paul

Additional information is available at the end of the chapter

<http://dx.doi.org/10.5772/61703>

Abstract

This chapter aims to familiarize readers with general knowledge of passive Q-switched and mode-locked fiber lasers. It emphasizes on carbon-based saturable absorbers, namely graphene and carbon nanotubes (CNTs); their unique electronic band structures and optical characteristics. The methods of incorporating these carbon-based saturable absorbers into fiber laser cavity will also be discussed. Lastly, several examples of experiments where carbon-based saturable absorbers were used in generating passive Q-switched and mode-locked fiber lasers are demonstrated.

Keywords: Fiber laser, passive Q-switch, passive mode-lock, graphene, carbon nanotube

1. Introduction

Graphene and carbon nanotubes are carbon allotropes that have a lot of interesting optical properties, which are useful for fiber laser applications. For instance, both allotropes have broadband operating wavelength, fast recovery time, are easy to fabricate, and can be integrated into fiber laser cavity. As a result, they can function as saturable absorber for generating Q-switching and mode-locking pulses. There are several techniques of incorporating these carbon-based saturable absorbers into fiber laser cavity. This chapter will discuss the advantages and disadvantages of most of the techniques that have been used.

2. Introduction to passive Q-switched and mode-locked fiber laser

2.1. Q-switched fiber lasers

A laser could emit short pulses if the loss of an optical resonator is rapidly switched from a high to a low value. By controlling the Q -factor (quality factor) of a laser resonator, Q -switching allows the generation of laser pulses of short duration (from nanosecond to picosecond range) and high peak power. The Q -factor (dimensionless) is given by:

$$Q = \frac{2\pi f_0 \varepsilon}{P} \quad (1)$$

where f_0 is the resonant frequency, ε is the stored energy in the cavity, and $P = -\frac{dE}{dt}$ is the power dissipated. If the Q -factor of a laser's cavity is abruptly changed from a low value to a high value, the laser will emit a pulse of light that is much more intense than the lasers' continues output. This technique is called Q -switching. There are two types of Q -switching; active and passive.

Active Q -switching uses modulation devices that change the cavity losses in accordance with an external control signal. They can be divided into three categories: mechanical, electro-optical, and acousto-optics. They inhibit laser action during pump cycle.

In passive Q -switching, the laser consists of gain medium and saturable absorber. The saturable absorber absorbs light at low intensity and transmits them at high intensity. As the gain medium is pumped, it builds up stored energy and emits photons. After many round-trips, the photon flux begins to see gain, fixed loss, and saturable loss in the absorber. If the gain medium saturates before the saturable absorber, the photon flux may build, but the laser will not emit a short and intense pulse. On the contrary, if the photon flux builds up to a level that saturates the absorber before the gain medium saturates, the laser resonator will see a rapid reduction in the intracavity loss and the laser Q -switches and therefore, will emit a short and intense pulse of light [1].

2.2. Mode-locked fiber laser

Mode-locking is a technique of generating an ultra-short pulse laser with pulse duration ranges from picoseconds (10^{-12} s) to femtoseconds (10^{-15} s). An ultra-short pulse can be generated when all the longitudinal modes have a fixed phase relationship. The fixed phase superposition between all the modes oscillating inside a laser cavity causes the cw laser to be transformed into a train of mode-locking pulse. The number of longitudinal mode that can simultaneously lase is dependent on the gain linewidth, $\Delta\nu_g$ and the frequency separation between modes. Under sufficiently strong pumping, we can expect that the number of modes oscillating in the cavity is given by:

$$M = \frac{\Delta\nu_g}{c/2L} = \frac{2L}{c} \Delta\nu_g \quad (2)$$

where c is the speed of light and L is the length of a linear cavity. The shortest pulse duration that we can expect to obtain by a given gain line width is:

$$\tau_{min} = \tau_M = \frac{2L}{cM} = \frac{1}{\nu_g} \quad (3)$$

From Eq. (3), we can conclude that the shortest pulse that can be obtained is a reciprocal of gain line width (in Hz) [2]. Depending on fiber laser cavity type, the fundamental repetition rate of a mode-lock fiber laser is determined by its cavity length, as shown in the equations below:

$$\text{Repetition rate (for linear cavity)} = \frac{c}{2Ln} \quad (4)$$

$$\text{Repetition rate (for ring cavity)} = \frac{c}{Ln} \quad (5)$$

where L , c and n denotes the length of the cavity, speed of light, and refractive index respectively. As the round-trip time, T_R is the inverse of repetition rate, therefore,

$$T_R = \frac{Ln(\text{ring cavity}) \text{ or } 2Ln(\text{linear cavity})}{c} \quad (6)$$

Under certain conditions, the repetition rate can be some integer multiple of the fundamental repetition rate. In this case, it is called harmonic mode-locking.

Mode-locking techniques can be divided into three categories; active, passive and hybrid. Active mode-locking can be achieved by using active modulator, e.g., acousto-optic or electro-optic, Mach-Zehnder integrated-optic modulator or semiconductor electro-absorption modulator. Passive mode-locking incorporates saturable absorber (SA) into the laser cavity. An artificial saturable absorber action can also be induced artificially by using Nonlinear Polarization Rotation (NPR) technique or by using another technique called Nonlinear Amplifying Loop Mirror (NALM). In comparison, the loss modulation of an active mode-locking is significantly slower due to its sinusoidal loss modulation. As with active mode-locking, a passive mode-locked pulse is much shorter than the cavity round-trip time. Hybrid mode-locking combines active and passive mode-locking. Hybrid mode-locking uses active modulator to start mode-locking while passive mode-locking is utilized for pulse shaping.

Many nonlinear systems exhibit an instability that result in modulation of the steady state. This is due to the interplay between the nonlinear and dispersive effects. This phenomenon is referred to as the *modulation instability*. In the context of fiber optics, modulation instability

requires anomalous dispersion and reveals itself as breakup of the cw or quasi-cw radiation into a train of ultrashort pulses [3-5]. The instability leads to a spontaneous temporal modulation of the cw beam and transforms it into pulse train [6].

There are many types of passive mode-locking pulses. However, for the sake of brevity, in this section, we will only discuss the soliton mode-locking pulse. It refers to a special kind of wave packets that can propagate undistorted over long distances. Soliton phenomena is formed by the interplay between the dispersive and nonlinear effects in a fiber laser cavity. Soliton mode-locking implies that the pulse shaping is solely done by soliton formation; the balance of group velocity dispersion (GVD) and self-phase modulation (SPM) at steady state. The mode-locking mechanism is not critically dependent on cavity design and no critical cavity stability regime is required. Soliton mode-locking basically works over the full cavity stability range.

In soliton mode-locking, an additional loss mechanism such as saturable absorber is essential to start the mode-locking process as well as stabilize the soliton pulse-forming process. In soliton mode-locking, the net gain window can remain open for more than 10 times longer than the ultrashort pulse, depending on the specific laser parameter [7, 8]. A stable soliton pulse is formed for all Group Delay Dispersion (GDD) values as long as the continuum loss (energy loss) is larger than the soliton loss [8] or the pulses break up into two or more pulses [9].

Soliton mode-locking can be expressed by using the following Haus master equation formalism [8, 10, 11]:

$$\sum_i \Delta A_i = \left[-iD \frac{\partial^2}{\partial t^2} + i\delta_L |A(T,t)|^2 \right] A(T,t) + \left[g - l + D_g \frac{\partial^2}{\partial t^2} - q(T,t) \right] A(T,t) = 0 \quad (7)$$

Here, $A(T, t)$ is the slowly varying field envelope, D is the intra-cavity GDD, $D_g = g / \Omega_g^2$ is the gain dispersion and Ω_g is the Half-Width of Half-Maximum (HWHM) of gain bandwidth. The SPM coefficient δ is given by $\delta = (2\pi / \lambda_0 A_L) n_2 \ell_L$, where n_2 is the intensity dependent refractive index of the gain medium, λ_0 is the center wavelength of the pulse, and A_L and ℓ_L is the effective mode area in the gain medium and length of light path through the gain medium within one round-trip, respectively. g is the saturated gain and l is the round-trip losses. $q(T, t)$ is the response of the saturable absorber due to an ultrashort pulse.

This soliton pulse propagates without distortion through a medium with negative GVD and positive SPM. The positive effect of SPM cancels the negative effect of dispersion. Kelly sidebands can usually be found in the optical spectrum of a soliton mode-locked fiber laser. A pronounced Kelly sidebands is an indicator that the mode-locked fiber laser is operating in its optimal pulse duration [12, 13].

3. Carbon-based saturable absorbers

Graphene and CNT have been used in Q-switching and mode-locking fiber lasers since 2003 [14-16] and 2009 [17], respectively. Compared to SESAM (Semiconductor Saturable Absorber

Mirror), CNT and graphene holds several advantages, e.g., broadband operating bandwidth, simple and low-cost fabrication process, and moderate damage threshold [18]. In this section, both electronic and optical characteristics of graphene and CNT are discussed in detail.

3.1. Graphene

3.1.1. *Electronic and band structure of graphene*

Graphene is the name we gave to a one-atom thick sp^2 hybridized carbon. It has a honeycomb-like structure. The sp^2 hybridization between s, p_x and p_y atomic orbitals create a strong covalent sp^2 bonds. The p_z orbital overlaps with other carbons to create a band of filled π orbitals. These bands have a filled shell and, therefore, form a deep valence band. On the other hand, the empty π^* orbitals are called the conduction band [19, 20].

Further observation of the band structure of graphene reveals three electronics properties that sparked such interest; the vanishing carrier density at Dirac point, the existence of pseudo-spin, and the relativistic nature of its carriers. The valance and conduction bands meet at high symmetry K points. Because the conduction and valence band meet at a symmetry K point, graphene is considered as zero-gap semiconductors (or zero-overlap semimetals) [21]. In intrinsic graphene, each carbon atom contributes one electron completely filling the valance band and leaving the conduction band empty. Therefore, the Fermi level, E_F , is situated precisely where the conduction and valence bands meet. These are known as the Dirac or charge neutrality points.

As mentioned before, due to this unique band structure of graphene, the following are three important features which to a large extent define the nature of electron transport of this material, namely, the zero-gap semiconductor, the existence of pseudo-spin, and the linear dispersion relation.

3.1.2. *Optical properties of graphene*

Graphene has three types of optical properties. They are linear optical absorption, saturable absorption, and luminescence. For generating passive Q-switch and mode-locked fiber lasers using graphene saturable absorber, our main interest is in the optical absorption and saturable absorption properties that graphene has.

Graphene saturable absorber has an ultrawide band operating wavelength as a result of its linear dispersion relation. Graphene only reflects <0.1% of the incident light in the visible region, increasing to ~2% for ten layers. Therefore, we can assume that the optical absorption of graphene layers is relative to the number of layers, for each layer absorbing $\approx 2.3\%$ over the visible spectrum [22].

The saturable absorption property of graphene is the result of Pauli blocking. Inter-band excitation by ultrafast optical pulses produces a nonequilibrium carrier population in the valence and conduction bands. In time-resolved measurements [23], two relaxation timescales are observed; a faster one of ~100 fs and a slower one, on picosecond timescale. The faster

relaxation time is related to the carrier–carrier intra-band collisions and phonon emission. The slower relaxation time corresponds to electron inter-band relaxation and cooling of hot phonons [24, 25]. For generating mode-lock laser, a saturable absorber with relaxation time in the timescale of \sim ps is necessary. In principle, single-layer graphene can provide the highest saturable absorption [26-28].

Graphene can be made luminescent by inducing a bandgap through two techniques to modify the electronic structure of graphene. One technique is by cutting it into ribbons and quantum dots [29] and the other is by chemical or physical treatments [30, 31], to reduce the connectivity of the π -electron network. A mild oxygen plasma treatment can make individual graphene flakes luminescent. The combination of photo-luminescent and conductive layers could be used in sandwich light-emitting diodes. Luminescent graphene-based material has been made to cover the infrared, visible, and blue spectral ranges [32-35].

3.2. Carbon nanotube

3.2.1. Electronic and band structure of carbon nanotube

The band structure of CNT can be assumed under a simple tight-binding model of [36]. In the model, CNT is considered as a roll of graphene layers. A very small change in diameter of the curvature of the fiber can affect the hybridization of sp^3 orbitals in which the electronic structure will also be affected. Therefore, the electronic structure depends on the geometry of the fiber and the fiber diameter.

The chiral vector, $\vec{C}_h \equiv (n, m)$, determines whether the CNT is metallic or semiconducting with bandgap. If $n - m = 3k$ (k is integer), the CNT is metallic, while when $n - m \neq 3k$, it shows that the CNT is semiconducting. At first, it was thought that the electrical and optical bandgaps of semiconducting CNTs were identical based on single particle model; however, the optical bandgap is actually smaller [37].

3.2.2. Optical properties of carbon nanotube

Just like graphene, CNT has several interesting optical properties. They are: optical absorption, saturable absorption, and electroluminescence and photoluminescence. The semiconducting CNTs have peak absorption wavelength depending on the optical bandgaps. Typical CNT with diameter d , of 7-15 nm has a bandgap energy of 1.2-0.6 eV, corresponds to the optical wavelength of 1–2 μ m. Thus, the peak absorption can be tuned by choosing the appropriate diameter. However, since CNTs are a mixture of several or many kinds of semiconducting and metallic CNT as well as different diameter distribution, the absorption peak is determined by the mean tube diameter and the absorption bandwidth depends on the tube diameter distribution. Although CNT is essentially a rolled-up graphene, the absorption of CNT is nonlinear. The optical absorption in CNT is anisotropic because CNT only absorbs the light whose polarization is parallel to the axial direction of the tube; therefore, an aligned CNT sample is polarization-dependent [38]. In spite of this, since we use a randomly oriented CNT samples, the CNT is polarization-independent [39].

Single-walled carbon nanotubes (SWCNTs) have been utilized as saturable absorber (SA) for mode-locking fiber laser long before graphene. The first publication of SWCNT SA can be traced as early as 2003 [15]. CNT can saturate with high-intensity light when the states of conduction band become full and the states at valence band become empty. Furthermore, the recovery time τ is observed to be very fast. In semiconducting CNT, the recovery time of E_{11} transition is an order of 1 ps, and the transition of E_{22} is in the order of 100 fs. Slower recovery in an order of several ps is also seen in the E_{11} transition. Several mechanisms believed to be responsible for the fast relaxation have been proposed. These mechanisms multi-phonon emission [40], tube–tube interaction [41], and exciton–exciton annihilation [42, 43].

The direct bandgap that exists in CNTs suggests that they can be efficient light absorbers and emitters. Studies regarding electroluminescence properties of SWCNT–polymer composites have been performed [44, 45]. Electron and hole carriers in semiconductors can recombine by different sorts of mechanisms. In most of the cases, the energy will be released as heat. Nevertheless, a fraction of the recombination events may involve the emission of a photon. The process is called electroluminescence and is responsible for producing solid-state light sources such as light-emitting diodes (LED). The direct bandgap of a semiconducting CNT is responsible for the photoluminescence phenomena in CNT. An electron in a CNT absorbs excitation light via transition from v_2 to c_2 and creates another excitation [46]. Electron and hole rapidly relax from c_2 to c_1 and from v_2 to v_1 states, respectively. Luminescence can only be observed in isolated semiconducting CNTs because the bundled CNTs have rapid transfer process from semiconducting to metallic CNTs [47]. Additionally, a semiconducting CNT can function as a nanoscale photodetector that converts light into current or voltage [48].

4. Preparation and fabrication of carbon-based saturable absorber

4.1. Optical deposition technique

In optical deposition technique, an intense light is injected into a CNT/ graphene-dispersed solution from a fiber-optic end to attract the CNT/graphene particle onto the ferrule tip [49-54]. There are generally two types of effects that lead to self-channeling of light in fluid suspension; the optical gradient force and thermal effects relying on (weak) absorption. When the particle size is smaller than the optical wavelength, the optical gradient force is weak; therefore, a higher particle density is required to cause significant change in the refractive index to trap narrow beams. With higher particle density, multiple scattering dominates; in-turn the direction of scattered light becomes random. This effect pushes the particles toward the beam center. Self-trap through very narrow beam is difficult because it requires high particle densities and this, in turn, involves multiple scattering, which acts as effective loss. Thermal effect can lead to a significant refractive index change, but in liquid, the refractive index typically decreases with increasing temperature [55].

Thermophoresis is a thermal mechanism that is often observed in colloidal suspension, which uses a strong reaction of the suspended particles to temperature gradients. Also known as the Soret effect, thermophoresis describes the ability of a macromolecule or particle to drift along

a temperature gradient [55]. Although various mechanisms are capable of depositing carbon-based saturable absorber to the fiber core, [52] has considered thermophoresis as the most likely process that is responsible for creating carbon-based saturable absorber via optical deposition. When the laser is turned on with the fiber in the solution, a strong convection current centered at the tips is observed. The induced current moves the carbon-based particles upward toward the fiber tip.

When fabricating a carbon-based saturable absorber using optical deposition, one must start by dispersing the carbon-nanotube/graphene bundles through ultrasonification process. Centrifugation follows to separate the macroscopic flakes and the agglomerated carbon nanotube/graphene. Only the homogeneous part of the solution is used for optical deposition process [49]. For depositing the carbon-based particles to the fiber core, precise optical power is essential. Lower optical power will not make the carbon-based particles adhere to the fiber core, while higher optical power will concentrate the deposition to the area around the fiber core. The difference between optimal and higher optical power is 1 dB [53]. The optimum optical power is influenced by other factors such as the size of particles, solution temperature, concentration levels of the solution, and the optical wavelength used in the deposition process [49, 53, 54]. For monitoring the optical deposition process, [50] has devised a setup that involves optical circulator and power meters. For controlling the insertion loss, the duration of the deposition has to be observed. Long deposition duration would create higher insertion loss.

Optical deposition technique is highly efficient as it only uses a small/required amount of carbon nanotube/graphene as saturable absorber. However, the disadvantages of this technique are large scattering loss [39], and the process itself is quite tedious as many factors can influence the required optical power in-order to make the carbon nanotube/graphene particles adhere to the fiber core. Furthermore, the success margin is small as only 1 dB can differentiate between optimal and high optical power.

4.2. Drop cast technique

Drop cast technique is simple and straightforward. Drip a graphene/SWCNT solution onto a fiber ferrule and let it dry to make an SA. This technique has been utilized in [56-58]. The SA insertion loss can be controlled depending on the concentration of the solution and the number of times this process is repeated. The process can also be repeated until the desired insertion loss is achieved.

Although the insertion loss is high, this can be overcome by increasing the pulse energy. As the pulse energy depends on the power and frequency, it can be altered by increasing pump power and/or lengthen the fiber laser cavity. The drawback of this technique is that in the course of increasing the pulse energy, we inevitably change the repetition rate and pulse width of the mode-locked fiber laser. Scattering loss is also an issue for this technique.

4.3. Mechanical exfoliation technique

Mechanical exfoliation uses scotch tape to repeatedly peel the graphene layers from a Highly Ordered Pyrolytic Graphite (HOPG) or graphitic flakes and transferring the layers to the

surface of the fiber ferrule. A fiberscope is normally used to examine that the graphene is transferred directly onto the core of the fiber ferrule. Mechanically exfoliated graphene SA has been demonstrated by [59-62] and [63]. The advantage of this technique is that it yields the best quality graphene SA. However, the drawback of this technique is that it is time-consuming. In addition, it could be difficult to control the desired graphene layer(s) that need to be transferred onto the core of the fiber ferrule.

4.4. Thin film and polymer composite

SWCNT and graphene thin films have been reported in many literatures [15, 17, 64]. For instance, [65] sprayed a liquid with dispersed CNTs onto a fiber end surface that acts as a substrate, while [15] sandwiched a thin layer of purified SWCNTs between two quartz substrates. CNTs and graphene polymer composite have also been demonstrated in numerous publications [26, 66-69]. Many kinds of polymer materials can be used as a host to graphene and CNTs, e.g., polymethylmethacrylate (PMMA), polyimide, and polycarbonate. The main advantages of using polymer composite as a host are that it reduces scattering and facilitates homogeneous dispersion of CNTs and graphene. It is thin enough to be sandwiched between fiber ferrules and has higher damage threshold compared to pure CNT/graphene layer. In spite of this, in terms of the amount used, it is less efficient than optical deposition technique and involves extra processing.

Other types of SA are also available, including tapered fiber [51, 70], D-shaped fiber [71], as well as CNT/graphene solutions embedded in photonic crystal fiber [72, 73].

5. Passive Q-switch and mode-lock experiments using carbon-based saturable absorbers

In this subsection, three pulsed Erbium-doped fiber lasers (EDFLs) are demonstrated using a comparatively simple and cost-effective carbon-based saturable absorber.

5.1. Passive Q-switch and mode-lock generation using Single-Walled Carbon Nanotubes (SWCNTs) saturable absorber via drop cast technique

Figure 1(a) shows the experimental setup for the proposed Q-switched EDFL, using a comparatively simple and cost-effective alternative technique based on SWCNTs SA. It consists of a 4 m long Erbium-doped fiber (EDF), two 1480/1550nm wavelength division multiplexers (WDM), an SWCNTs-based SA, an optical isolator, and a 20 dB output coupler in a ring configuration. The EDF is a commercial fiber with Erbium ion concentration of 2000 ppm, cut off wavelength of 920 nm, and numerical aperture of 0.24. It is backward pumped by a 1480 nm laser diode (LD) with the maximum output power of 129 mW via the WDM. Another 1480/1550 WDM is used after the gain medium to dispose excess power from the LD. An isolator is used to ensure unidirectional propagation of light inside the cavity. The homemade SWCNT SA is placed between the isolator and the WDM to act as a Q-switcher. The SWCNT SA was fabricated using the drop cast method.

The output of the laser is extracted from the cavity using the 1% output port of the optical coupler. An optical spectrum analyzer (OSA, AQ6317B) is utilized for the spectral analysis of the Q -switched EDFL, which has the spectral resolution set to 0.02 nm, whereas an oscilloscope (OSC, Tektronix, TDS 3052C) is used to monitor the pulse train of the Q -switched operation via coupling the oscilloscope with a 6 GHz bandwidth photo-detector. Total cavity length is 23 m. Except for the gain medium, the rest of the cavity uses a standard SMF-28 fiber. The total cavity length of the ring resonator is measured to be around 23 m. Furthermore, all optical components are polarization-independent.

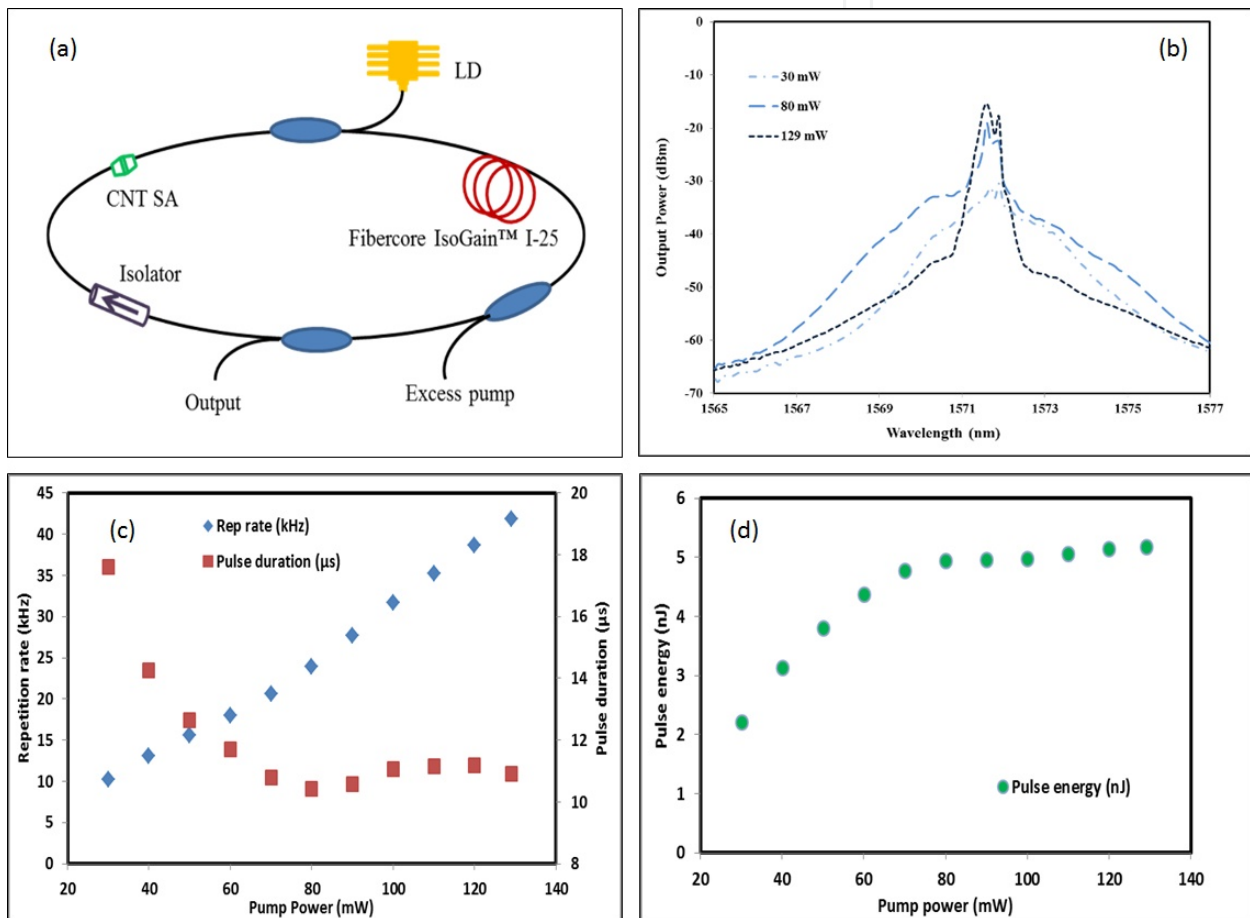


Figure 1. (a) Experimental setup for the proposed SWCNTs-based Q -switched EDFL. (b) Output spectra of the Q -switched EDFL at three different pump powers: 30 mW, 80 mW, and 129 mW. (c) Repetition rate and pulse duration relationship with pump power. (d) Pulse energy relationships with pump power.

Stable and self-starting Q -switching operation is obtained just by increasing the pump power over 30 mW. Figure 1(b) compares the output spectra of the EDFL at three different pump powers; 30 mW, 80 mW, and 129 mW. As shown in the figure, the laser operates at center wavelength of around 1571.6 nm. Spectral broadening is observed in the spectrum especially at a pump power of 80 mW, which corresponds to the minimum pulse width region. This is attributed to the Self-Phase Modulation (SPM) effect in the laser cavity [74]. The maximum

Full-Width at Half-Maximum (FWHM) of 0.6 nm is obtained when the pump power was increased to maximum (129 mW).

Figure 1(c) shows the relationship between repetition rates and pulse durations with pump power. As pump power increases from 30 mW to 129 mW, the repetition rate increases linearly from 10.25 kHz to 41.87 kHz. As pump power increases, more gain is provided to saturate the SA and thus increases repetition rate. In contrast, pulse duration decreases from 17.6 μs to 10.92 μs as the pump power increases. However, the lowest pulse duration of 10.42 μs is achieved at 80 mW pump power. After the pump power increases from 80 mW to 129 mW, the pulse durations increase slightly before decreasing back at 129 mW. Hence, the minimum attainable pulse duration is 10.24 μs , which is related to modulation depth of the saturable absorber [75, 76]. Based on the minimum attainable pulse duration, the modulation depth of the SWCNT SA is calculated to be around 3.7%. Figure 1(d) shows the relationship between pulse energy and pump power in the proposed Q-switched EDFL. As the pump power increases, the average output power also increases, which gives rise to pulse energy. It is obtained that the pulse energy can be increased from 2.23 nJ to 4.94 nJ by tuning the pump power from 30 to 80 mW, and from 4.94 nJ to 5.19 nJ when the pump power increases from 80 mW to 129 mW. The calculated average slope efficiency is 12% when the pump power increases from 30 mW to 80 mW. From 80 mW to 129 mW pump power, the calculated average slope efficiency is 16%. The pulse energy is saturated as the pump power is further increased above 80 mW.

5.2. Mode-locked erbium-doped fiber laser using Single-Walled Carbon Nanotubes (SWCNTs) saturable absorber via drop cast technique

In order to saturate the SA in a single-pass, the laser cavity is slightly changed compared to the previous subsection. The experimental setup for proposed SWCNTs-based mode-locked EDFL is shown in Figure 2(a). Compared to the previous setup, a 200 m long SMF is added in the mode-locked setup to reduce the repetition rate of the output pulse and thus increase the pulse energy in the cavity. This gives total cavity length of ~223 meter and a total Group Velocity Dispersion (GVD) of 3.6364 ps nm⁻¹. Therefore, the fiber laser is operating in the anomalous dispersion regime. For pulse duration measurement, an autocorrelator with 25 fs resolution was used. The SNR is measured using Anritsu MS2667C Radio Frequency Spectrum Analyzer (RFSAs).

Soliton mode-locking operation self-starts at 56.75 mW without Q-switching instabilities. It is observed that the pulse state diminishes into continuous-wave (CW) when the pump power is below 30 mW. The resultant repetition rate is 907 kHz, which corresponds to 1.1 μs round-trip time. Figure 2(b) shows output spectrum of the proposed mode-locked EDFL. As shown in the figure, the laser operates at a central wavelength, λ_C of 1570.5 nm with 3-dB bandwidth of 1.080 nm. Compared to the Q-switched laser, the mode-locked laser operates at a shorter wavelength due to the incorporation of 200 m long SMF in the cavity, which increases the cavity loss. The operating wavelength shifts to shorter wavelength to acquire more gain to compensate the loss.

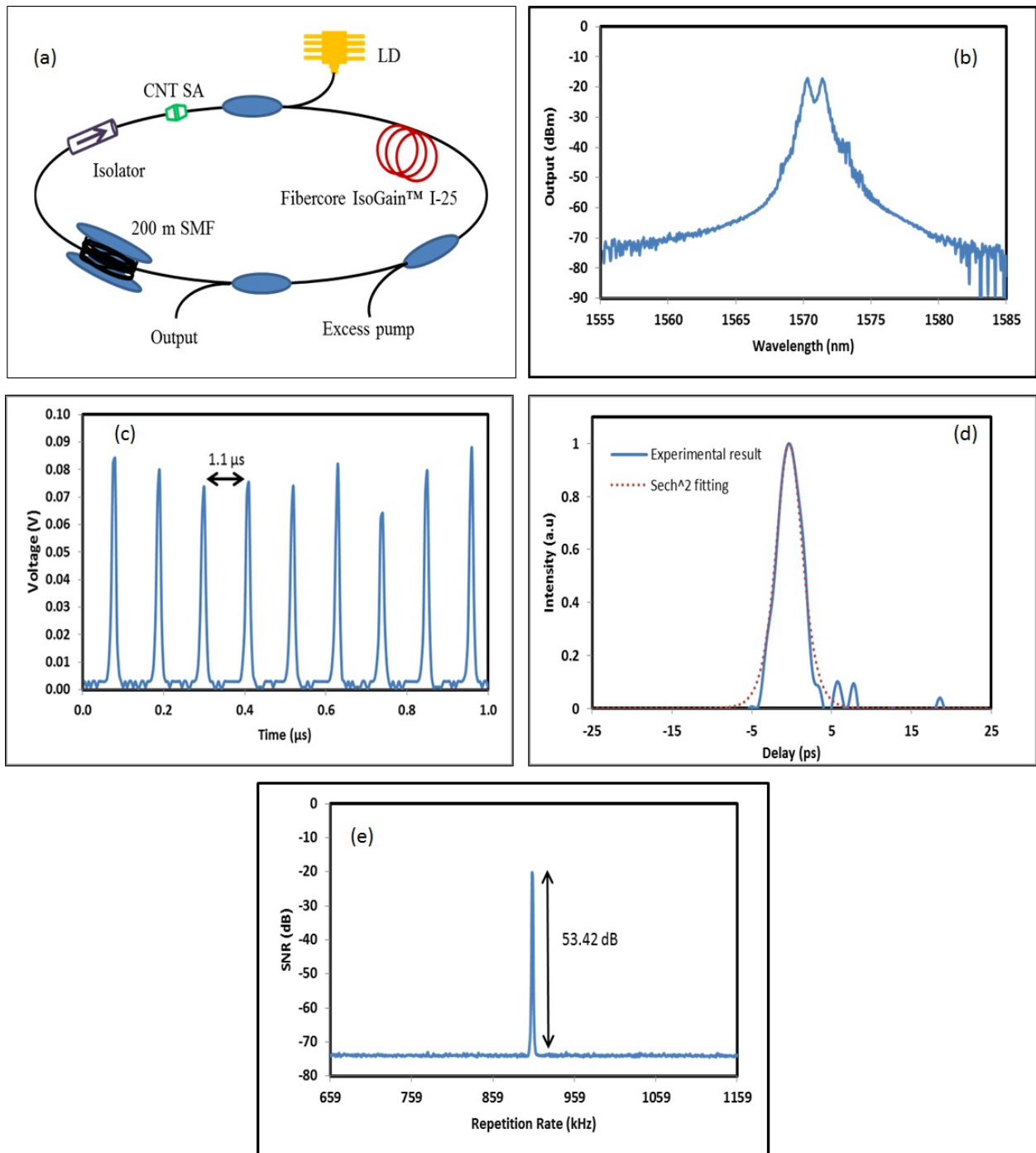


Figure 2. (a) Experimental setup for soliton mode-lock operation. (b) Output spectrum of the proposed soliton mode-locked EDFL when the pump power is fixed at 129 mW. (c) OSC trace of mode-locked fiber laser (d) Autocorrelation trace of mode-locked fiber laser at 129 mW. (e) RFSA trace of soliton mode-locked fiber laser at 129 mW.

Figure 2(c) shows the typical pulse train of the mode-locked EDFL at pump power of 129 mW. Figure 2(d) shows the corresponding autocorrelation trace of the mode-locked pulse showing the pulse duration, T_{FWHM} of 2.52 ps. The RF spectrum of the mode-locked laser is also investigated using a RF spectrum analyzer. Figure 2(e) shows the result, which indicates a

strong mode-locked pulse at frequency of 907 kHz. Figure 2(e), SNR is obtained at 53.42 dB, which is limited by the available pump power. The average output power of the soliton mode-locked fiber laser is measured to be -6.54 dBm. Based on the 3 dB bandwidth of the output spectrum, a Time Bandwidth Product (TBP) of laser is calculated to be around 0.331, which shows that the soliton pulse is slightly chirped.

Referring to Figure 2(d), the autocorrelation trace does not follow exactly the sech^2 fitting. When mode-locked pulse self-starts at 56.75 mW, the pulse shape does follow exactly the shape of the sech^2 fitting. However, in the RFSA, the SNR value is below the threshold value required to be qualified as mode-locked pulse. This is due to the 20 dB output coupler used in the experimental setup. Only 1% of the total energy that is circulating inside the cavity is extracted for measurement purpose.

Therefore, the pump power is increased to 129 mW to achieve a satisfactory SNR value. However, this, in turn, increases the pulse intensity in the autocorrelator. As a result, the pulse shape in the autocorrelator does not follow the sech^2 fitting.

5.3. Passive Q-switched fiber laser generation using graphene saturable absorber

Graphene was first produced by a mechanical exfoliation method in 2004 [77]. In this work, a fresh surface of a layered crystal was rubbed against another surface, which left a variety of flakes attached to it. Among the resulting flakes, a single layer flake can be found. Despite there being other methods to produce graphene, mechanical exfoliation still gives the best samples in terms of purity, defects, electron mobility, and optoelectronic properties. A single-layer graphene saturable absorber has an ultrafast relaxation time, lower scattering loss, and it performs better than multilayer graphene saturable absorber in terms of pulse-shaping ability, pulse stability, and output energy [28]. However, this method has disadvantages in terms of yield and throughput, and thus it is impractical for large-scale production. Graphene can be optically distinguished, regardless of being one-atom thick and its transmittance (T) can be expressed in terms of the fine-structure constant. Due to some properties of graphene such as linear dispersion of the Dirac electrons and Pauli blocking, it makes broadband applications and saturable absorption possible [35]. In this section, the preparation of a single-layer graphene SA (GSA) based on mechanical exfoliation technique, also known as the “scotch tape” method, is demonstrated. The position of graphene SA on the fiber core can easily be recognized by using a fiber probe.

The material is a commercially available, highly ordered pyrolytic graphite (HOPG). An HOPG flake was inserted on a strip of scotch tape and then were pressed and peeled off repeatedly in order to reduce the graphene layers to a single layer. The resultant graphene layers were then pressed against the end facet of an optical fiber ferrule in order to transfer it. The scotch tape was slowly peeled off and subsequently, a few graphene layers stick on the optical fiber ferrule. Graphical presentation of this technique is explained in detail by [60]. The result is inspected using EXFO's FIP-400 fiber inspection probe to ensure that the graphene sheets lie on top of the fiber core. The microscope image of the end surface of the ferrule after coating the graphene is illustrated in Figure 3.

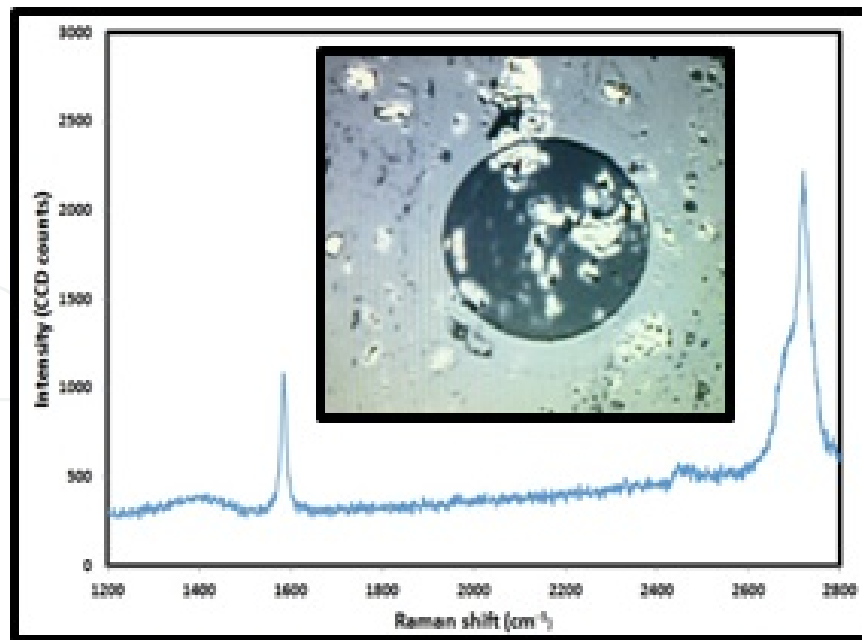


Figure 3. Raman Spectrum of the GSA. Fiberscope image of fiber ferrule with graphene (inset).

The setup of the proposed Q -switched EDFL with the newly developed GSA is similar to the previous section, except for the gain medium, SA, and 200 m long fiber. It is based on unidirectional ring cavity configuration consisting of two wavelength division multiplexer (WDM) coupler, 49 cm long bismuth-based Erbium-doped fiber (Bi-EDF) as gain medium. Since there is no polarizer in the laser cavity, the graphene is the sole responsible mechanism for creating saturable absorption.

In the experiment, the continuous wave (CW) lasing threshold was about 30 mW. When the pump power was increased to about 80 mW, the Q -switched pulses were observed by introducing physical disturbance to the cavity. Then, the pump power is further increased to the maximum pump power of 130 mW and observed the Q -switched operation. Figure 4(a) shows the output spectrum of the Q -switched EDFL at 130 mW pump power. A slight spectral broadening is also observed in the optical spectrum, which is caused by Self-phase Modulation effect (SPM). Correspondingly, the typical Q -switched pulse train is presented in Figure 4(b). As shown in the figure, the peak-to-peak pulse interval is measured to be around 43.3 μ s, which can be translated into repetition rate of 26 kHz. At 130 mW pump power, the Q -switched laser has an average output power of 0.5656 mW, which corresponds to pulse energy of 24.399 nJ.

Figure 4(c) represents the pulse repetition rate and the pulse energy of the Q -switched fiber laser as a function of the pump power. The repetition rate can be tuned from 16.7 kHz to 23.1 kHz by increasing the pump power. The attainable energy is lower than the previous Q -switched laser with optical deposition technique based GSA. This is attributed to the large modulation depth of the single-layer graphene SA. A large modulation depth implies a large change in absorption for the incident light. Therefore, a lower repetition rate and pulsewidth are achieved with higher modulation depth [78].

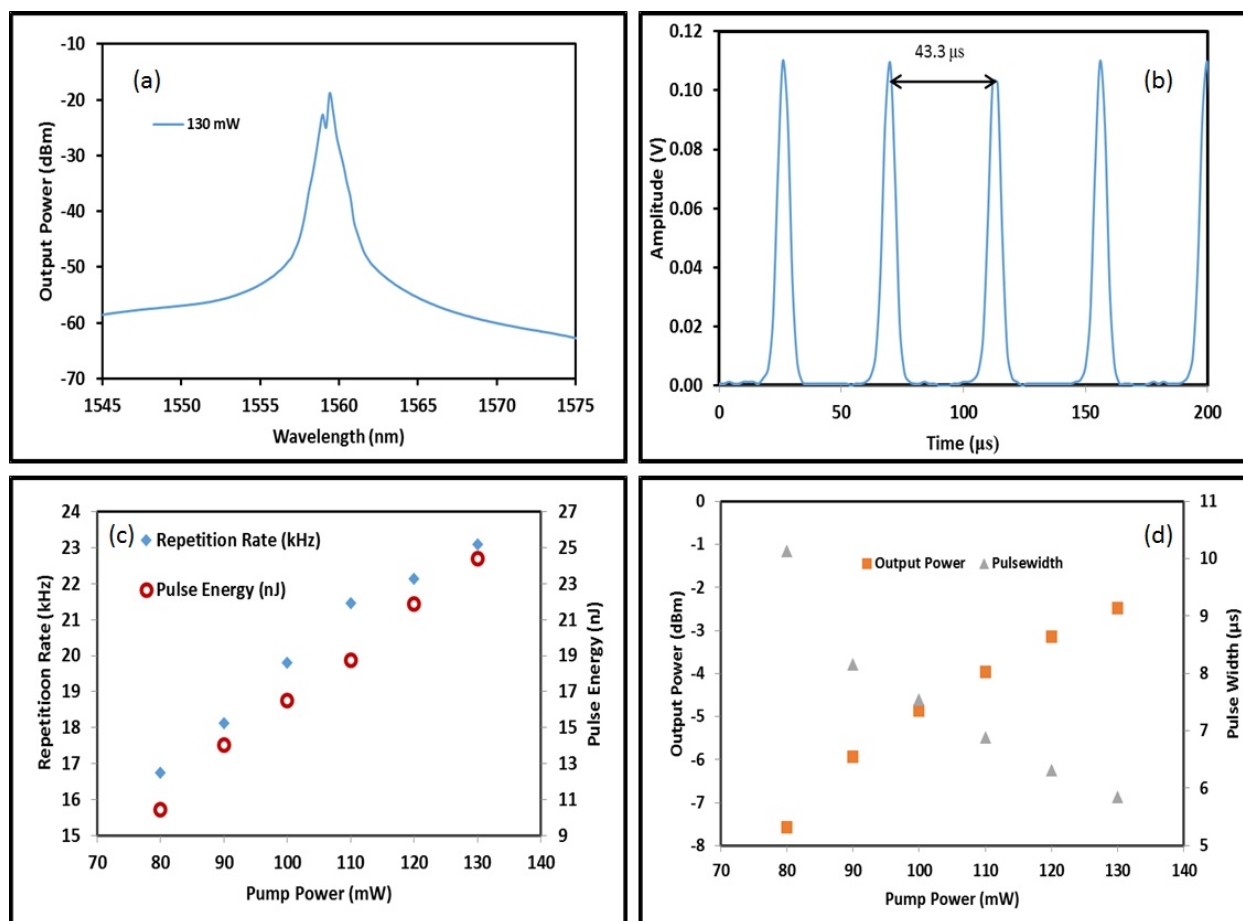


Figure 4. (a) Optical spectrum of the Q-switched laser at pump power of 130 mW. (b) Pulse train of the Q-switched laser at 130 mW pump power. (c) Repetition rate and pulse energy as a function of pump power. (d) Output power and pulse width as a function of pump power.

5.4. Passive mode-locked fiber laser using graphene saturable absorber

Figure 5(a) shows the modified configuration where a longer EDF is used in conjunction with an additional 200 m long SMF-28 to reduce the repetition rate and increase the pulse energy. The length of total cavity is about 207 m, including 1.6 m EDF, 205.4 m SMF-28 fiber from the WDM, isolator, coupler, and additional spool of SMF. The net GVD in the cavity was calculated to be 3.457 ps/nm, confirming that the laser was operating at an anomalous dispersion regime.

The mode-locking operation is not self-started in the proposed setup. Stable mode-locked pulses were observed as shown in Figure 5(b) by introducing physical disturbance to the SA after increasing the 1480 nm pump power to the maximum (130 mW). The mode-locking pulse then disappears when pump power falls below 84.5 mW. As shown in Figure 5(b), the cavity round-trip time is measured to be 1.034 μs, which corresponds to repetition rate of 967 kHz.

Figure 5(c) shows the measured optical spectrum of the soliton pulses at the launched pump power of 130 mW. Although the resultant pulse fiber laser is a soliton mode-locked fiber laser, Kelly sidebands are less prominent due to excessive nonlinearity caused by high pump power and cavity length [12]. Figure 5(d) shows the measured interference autocorrelation trace of

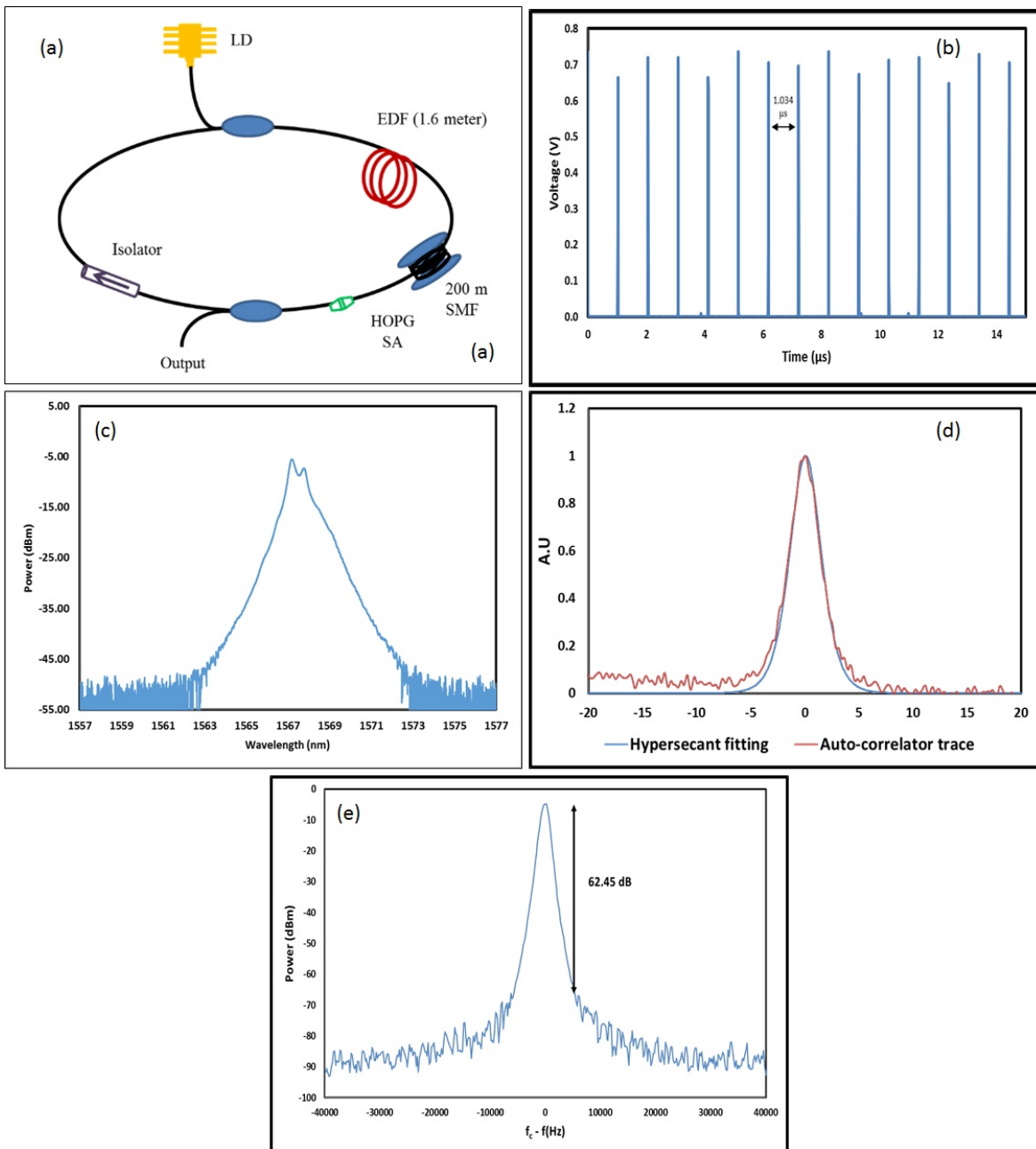


Figure 5. (a) Configuration of the mode-locked EDFL with GSA. (b) Typical mode-locking pulse train on oscilloscope. (c) OSA trace of the mode-locked EDFL. (d) Autocorrelation trace of the mode-locking pulse at launched pump power of 130 mW. (e) RF spectrum of the mode-locked pulse train.

the mode-locked pulses at a scanning range of 40 ps. As shown in Figure 5(d), the pulse was very well fitted by a sech^2 pulse profile, and the pulse duration was measured to be 3.41 ps. Consequently, the TBP was calculated to be 0.38, which is almost 1.2 times larger than the ideal TBP value (0.315). This is most probably due to the large GVD in the laser cavity and high pump power. Figure 5(e) shows the RF spectrum of the output at the launched pump power of 130 mW. The SNR of 62.45 dB indicated that the oscillator operated at stable mode-locking regime.

5.5. Passive mode-locked fiber laser using nonconductive graphene oxide paper

Figure 6 shows the result of Raman spectroscopy on graphene oxide paper. The spectroscopy was performed using a 532 nm laser with only 10% power and exposure time was set to 20 s. From the result, there are two distinctive peaks that can be observed; at 1349 cm^{-1} and 1588 cm^{-1} . These two peaks are D-band and G-band, respectively [79]. The excitation at D-band is caused by the hybridized vibrational mode related to graphene edges, and it also shows a disorder in the graphene structure. The graphite or tangential band (G-band) exists due to the energy in the sp^2 bonded carbon in planar sheets. The in-plane optical vibration of the bond resulted in Raman spectrum at the mentioned frequency [80]. A small peak at 2700 cm^{-1} , which is also known as G' or 2D band, is barely observable because the laser power is low. The graphene layers can be indicated by the ratio of G' and G bands. Because the intensity of G' band is lower than the G band, it also shows that the GO paper is more than one layer.

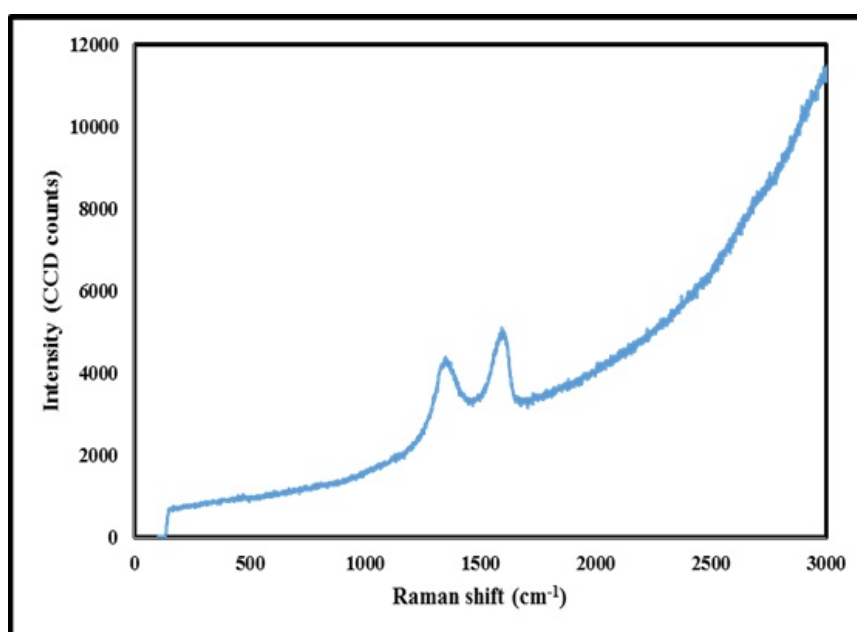


Figure 6. Raman spectroscopy result of graphene oxide paper.

The schematic of the proposed mode-locked EDFL is shown in Figure 7(a). It was constructed using a simple ring cavity, in which a 1.6 m long EDF with an Erbium ion concentration of 2000 ppm was used for the active medium and the GO paper SA was used as a mode-locker.

The SA was fabricated by cutting a small piece ($2 \times 2\text{ mm}^2$) of a commercially nonconductive graphene oxide paper [81] and sandwiching it between two FC/PC fiber connectors, after depositing index-matching gel onto the fiber ends. The thickness of the GO paper is $10\text{ }\mu\text{m}$, while the measured insertion loss of the SA to be 1.0 dB at 1550 nm. The total length of the laser cavity was measured to be approximately 12.6 meter. The resultant total GVD for this mode-locked fiber laser was calculated to be 0.1513 ps/nm . This indicated that the proposed mode-locked fiber laser operated in the anomalous dispersion regime and thus it could be classified as a soliton fiber laser.

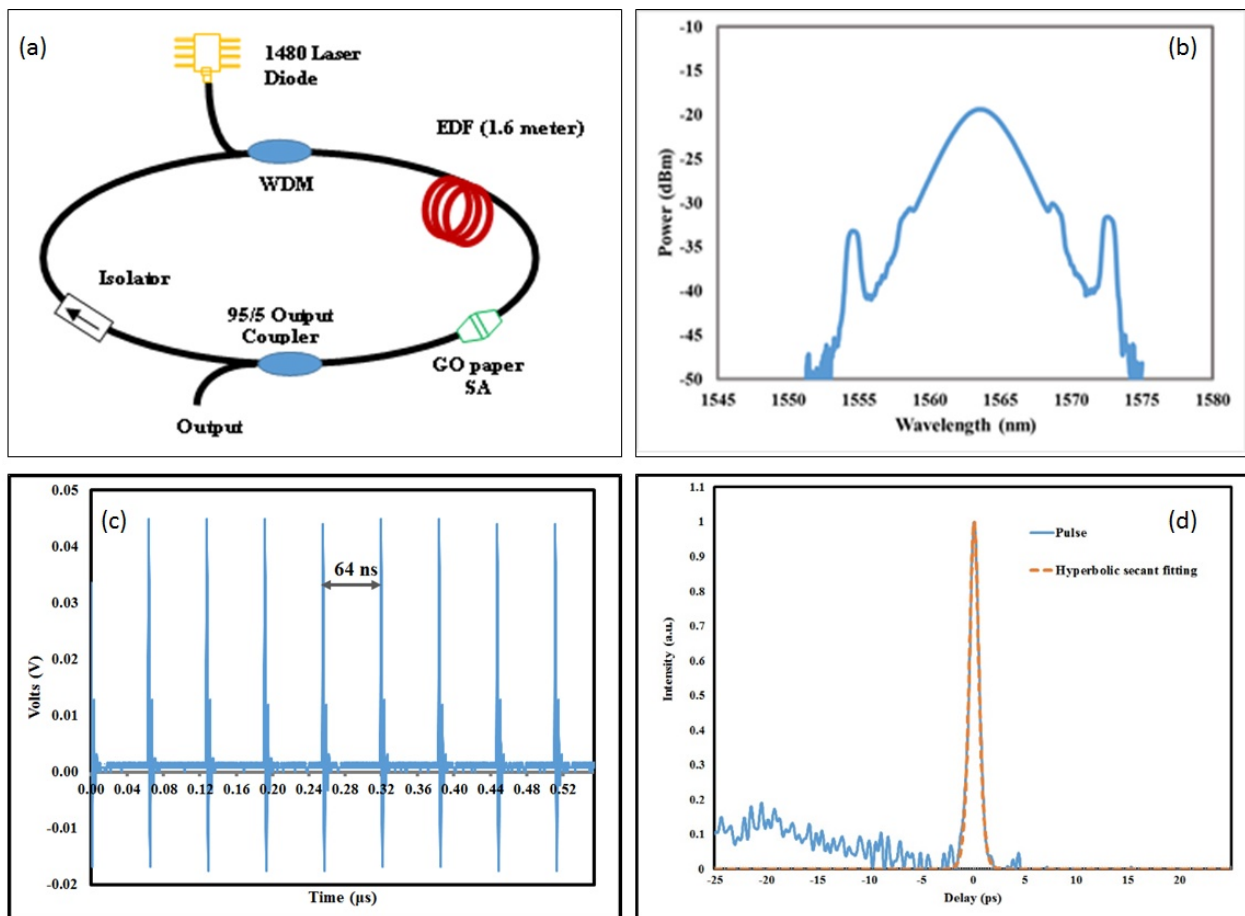


Figure 7. (a) Experimental setup. (b) Spectral characteristic of mode-locked fiber laser using GO paper. (c) Mode-locked pulse train with cavity round-trip time. (d) Autocorrelation trace.

The mode-locked fiber laser had a low self-starting threshold; approximately at 17.5 mW. Before all the modes were locked, multiple pulsing could be seen to occur at pump power as low as 10 mW. Figure 7(b) shows the spectral profile where the presence of soliton is confirmed. The presence of Kelly sidebands confirms that this mode-lock fiber laser is operating in anomalous dispersion regime. Figure 7(c) shows the pulse train of the passive mode-locked fiber. It has a cavity round-trip time of 64 ns, corresponding to a pulse repetition rate 15.6 MHz. Figure 7(d) shows the autocorrelation trace with measured pulsewidth of 680 fs at its FWHM. The sech^2 fitting, which indicates the generation of the soliton pulse, is also included in the figure. The autocorrelation trace reveals that the experimental result follows the sech^2 fitting closely. A TBP of 0.315 is calculated from the 3-dB bandwidth of the optical spectrum and the acquired pulsewidth. This shows that the pulse is a transform-limited pulse. Since the pulsing threshold is low, the output power for this fiber laser is 0.134 mW. Consequently, the resultant pulse energy and peak power are 0.0085 nJ and 11.85 W, respectively.

As the data measurements are performed, it is observed that the pulse increasingly expanded and the spectral profile gradually changed from soliton to laser. Therefore, it is suspected that the pulse gradually is destroying the SA. Moreover, at approximately 24.4 mW, the output power was attenuated. Thus, it is concluded that a 1-layer GO paper SA is only effective in a

short period of time and has low damage threshold. For the same reason, a satisfactory SNR data using RFSA is unable to be acquired. Together with low pulsing and damage thresholds, combined with the 5% of the intracavity energy taken out for performing measurements, it seems that the SNR is unable to extend more than 30 dB.

It is found that CNT and graphene saturable absorber may have inconsistent properties when prepared by different groups of researchers; despite repeating the same process. Currently, scientists are moving forward toward finding new materials that can be utilized as saturable absorber. The discovery of 2D material such as graphene has sparked interest in the potential of other 2D material. In recent developments, other 2D materials have been incorporated into fiber laser cavity to generate Q-switched and mode-locked fiber lasers. Topological insulator [19-22], transition metal dichalcogenides [23-25], and black phosphorus [26, 27] are among the recent materials being developed as saturable absorber.

6. Conclusion

We have discussed graphene and CNT saturable absorbers and their applications in generating passive Q-switched and mode-locked fiber lasers. We have demonstrated several examples of experiments where carbon-based saturable absorbers were used in generating Q-switched and mode-locked pulse in EDFL cavity. Currently, scientists are also moving forward toward new saturable absorber materials such as topological insulator and black phosphorus.

Acknowledgements

The authors acknowledge funding from the University of Malaya (Project Number: UM.C/625/1/HIR/MOE/ENG/09 and SF014-2014)

Author details

Mohd Afiq Ismail^{1*}, Sulaiman Wadi Harun², Harith Ahmad¹ and Mukul Chandra Paul³

*Address all correspondence to: afiq.ismail@siswa.um.edu.my

1 Photonics Research Centre, University of Malaya, Kuala Lumpur, Malaysia

2 Dept. of Electrical Engineering, Fac. of Engineering, University of Malaya, Kuala Lumpur, Malaysia

3 Fibre Optics Division, Central Glass and Ceramic Research Institute, Kolkata, India

References

- [1] Welford D. Passively Q-switched lasers. *Circuits and Devices Magazine, IEEE*. 2003;19(4):31-6.
- [2] Milonni P, Eberly J. *Lasers physics*. Hoboken. New Jersey: Wiley; 2010.
- [3] Hasegawa A. Generation of a train of soliton pulses by induced modulational instability in optical fibers. *Opt Lett*. 1984 Jul 1;9(7):288-90. PubMed PMID: 19721573.
- [4] Islam MN, Dijaili S, Gordon JP. Modulation-instability-based fiber interferometer switch near 1.5 μm . *Optics letters*. 1988;13(6):518-20.
- [5] Boyd RW, Raymer MG, Narducci LM. *Optical instabilities*. Cambridge University Press, New York, NY, 1986.
- [6] Agrawal GP. *Nonlinear fiber optics*: Springer; 2000.
- [7] Jung I, Kärtner F, Brovelli L, Kamp M, Keller U. Experimental verification of soliton mode locking using only a slow saturable absorber. *Optics letters*. 1995;20(18):1892-4.
- [8] Kärtner F, Jung I, Keller U. Soliton mode-locking with saturable absorbers. *Selected Topics in Quantum Electronics, IEEE Journal of*. 1996;2(3):540-56.
- [9] Au J, Kopf D, Morier-Genoud F, Moser M, Keller U. 60-fs pulses from a diode-pumped Nd: glass laser. *Optics letters*. 1997;22(5):307-9.
- [10] Duling III IN. *Compact sources of ultrashort pulses*: Cambridge University Press; 2006.
- [11] Kärtner FX, Keller U. Stabilization of solitonlike pulses with a slow saturable absorber. *Optics Letters*. 1995 1995/01/01;20(1):16-8.
- [12] Dennis ML, Duling III IN. Experimental study of sideband generation in femtosecond fiber lasers. *Quantum Electronics, IEEE Journal of*. 1994;30(6):1469-77.
- [13] Kelly S. Characteristic sideband instability of periodically amplified average soliton. *Electronics Letters*. 1992;28(8):806-7.
- [14] Set S, Yaguchi H, Tanaka Y, Jablonski M, Sakakibara Y, Tokomuto M, et al., editors. A dual-regime mode-locked/Q-switched laser using a saturable absorber incorporating carbon nanotubes (SAINT). *Lasers and Electro-Optics, 2003 CLEO'03 Conference on; 2003: IEEE*.
- [15] Set SY, Yaguchi H, Tanaka Y, Jablonski M, Sakakibara Y, Rozhin A, et al., editors. Mode-locked fiber lasers based on a saturable absorber incorporating carbon nanotubes. *Optical Fiber Communication Conference; 2003: Optical Society of America*.
- [16] Set SY, Yaguchi H, Jablonski M, Tanaka Y, Sakakibara Y, Rozhin AG, et al., editors. A noise suppressing saturable absorber at 1550nm based on carbon nanotube technology. *Optical Fiber Communication Conference; 2003: Optical Society of America*.

- [17] Bao Q, Zhang H, Wang Y, Ni Z, Yan Y, Shen ZX, et al. Atomic-Layer Graphene as a Saturable Absorber for Ultrafast Pulsed Lasers. *Adv Funct Mater.* 2009;19:3077-83.
- [18] Yamashita S, editor *Carbon-nanotube and graphene photonics2011*: Optical Society of America.
- [19] Neto AC, Guinea F, Peres N, Novoselov K, Geim A. The electronic properties of graphene. *Reviews of modern physics.* 2009;81(1):109.
- [20] Allen MJ, Tung VC, Kaner RB. Honeycomb Carbon: A Review of Graphene. *Chem Rev.* 2010;110(1):132-45. English.
- [21] Geim AK, Novoselov KS. The rise of graphene. *Nature materials.* 2007;6(3):183-91.
- [22] Nair R, Blake P, Grigorenko A, Novoselov K, Booth T, Stauber T, et al. Fine structure constant defines visual transparency of graphene. *Science.* 2008;320(5881):1308-.
- [23] Breusing M, Ropers C, Elsaesser T. Ultrafast Carrier Dynamics in Graphite. *Physical Review Letters.* 2009 02/27/;102(8):086809.
- [24] Lazzeri M, Piscanec S, Mauri F, Ferrari AC, Robertson J. Electron Transport and Hot Phonons in Carbon Nanotubes. *Physical Review Letters.* 2005 11/30/;95(23):236802.
- [25] Kampfrath T, Perfetti L, Schapper F, Frischkorn C, Wolf M. Strongly coupled optical phonons in the ultrafast dynamics of the electronic energy and current relaxation in graphite. *Physical review letters.* 2005;95(18):187403.
- [26] Sun Z, Hasan T, Torrisi F, Popa D, Privitera G, Wang F, et al. Graphene mode-locked ultrafast laser. *Acs Nano.* 2010;4(2):803-10.
- [27] González J, Guinea F, Vozmediano M. Unconventional quasiparticle lifetime in graphite. *Physical review letters.* 1996;77(17):3589-92.
- [28] Bao Q, Zhang H, Ni Z, Wang Y, Polavarapu L, Shen Z, et al. Monolayer graphene as a saturable absorber in a mode-locked laser. *Nano Research.* 2011;4(3):297-307.
- [29] Dössel L, Gherghel L, Feng X, Müllen K. Graphene Nanoribbons by Chemists: Nanometer-Sized, Soluble, and Defect-Free. *Angewandte Chemie International Edition.* 2011;50(11):2540-3.
- [30] Gokus T, Nair R, Bonetti A, Bohmler M, Lombardo A, Novoselov K, et al. Making graphene luminescent by oxygen plasma treatment. *ACS nano.* 2009;3(12):3963-8.
- [31] Stöhr RJ, Kolesov R, Pflaum J, Wrachtrup J. Fluorescence of laser-created electron-hole plasma in graphene. *Physical Review B.* 2010 09/14/;82(12):121408.
- [32] Eda G, Lin YY, Mattevi C, Yamaguchi H, Chen HA, Chen I, et al. Blue photoluminescence from chemically derived graphene oxide. *Advanced Materials.* 2010;22(4):505-9.

- [33] Sun X, Liu Z, Welsher K, Robinson JT, Goodwin A, Zaric S, et al. Nano-graphene oxide for cellular imaging and drug delivery. *Nano research*. 2008;1(3):203-12.
- [34] Lu J, Yang J-x, Wang J, Lim A, Wang S, Loh KP. One-Pot Synthesis of Fluorescent Carbon Nanoribbons, Nanoparticles, and Graphene by the Exfoliation of Graphite in Ionic Liquids. *ACS Nano*. 2009 2009/08/25;3(8):2367-75.
- [35] Bonaccorso F, Sun Z, Hasan T, Ferrari A. Graphene photonics and optoelectronics. *Nature Photonics*. 2010;4(9):611-22.
- [36] Saito R, Fujita M, Dresselhaus G, Dresselhaus MS. Electronic structure of graphene tubules based on C₆₀. *Physical Review B*. 1992;46(3):1804.
- [37] Wang F, Dukovic G, Brus LE, Heinz TF. The optical resonances in carbon nanotubes arise from excitons. *Science*. 2005;308(5723):838-41.
- [38] Song YW, Yamashita S, Einarsson E, Maruyama S. All-fiber pulsed lasers passively mode locked by transferable vertically aligned carbon nanotube film. *Optics letters*. 2007;32(11):1399-401.
- [39] Yamashita S. A Tutorial on Nonlinear Photonic Applications of Carbon Nanotube and Graphene. *Lightwave Technology, Journal of*. 2012;30(4):427-47.
- [40] Ichida M, Hamanaka Y, Kataura H, Achiba Y, Nakamura A. Ultrafast relaxation dynamics of photoexcited states in semiconducting single-walled carbon nanotubes. *Physica B: Condensed Matter*. 2002;323(1):237-8.
- [41] Tatsuura S, Furuki M, Sato Y, Iwasa I, Tian M, Mitsu H. Semiconductor carbon nanotubes as ultrafast switching materials for optical telecommunications. *Advanced Materials*. 2003;15(6):534-7.
- [42] Ma Y-Z, Hertel T, Vardeny ZV, Fleming GR, Valkunas L. Ultrafast spectroscopy of carbon nanotubes. *Carbon Nanotubes: Springer*; 2008. p. 321-52.
- [43] Ma Y-Z, Stenger J, Zimmermann J, Dexheimer SL, Fleming GR, Bachilo SM, et al., editors. Ultrafast carrier dynamics in single-walled carbon nanotubes probed by femto-second spectroscopy. *International Quantum Electronics Conference*; 2004: Optical Society of America.
- [44] Kazaoui S, Minami N, Nalini B, Kim Y, Takada N, Hara K. Near-infrared electroluminescent devices using single-wall carbon nanotubes thin films. *Applied Physics Letters*. 2005;87(21):211914--3.
- [45] Xu Z, Wu Y, Hu B, Ivanov IN, Geohegan DB. Carbon nanotube effects on electroluminescence and photovoltaic response in conjugated polymers. *Applied Physics Letters*. 2005;87(26):263118--3.
- [46] Bachilo SM, Strano MS, Kittrell C, Hauge RH, Smalley RE, Weisman RB. Structure-assigned optical spectra of single-walled carbon nanotubes. *Science*. 2002;298(5602):2361-6.

- [47] Gutsche C. S. Reich, C. Thomsen, J. Maultzsch: Carbon nanotubes, basic concepts and physical properties. *Colloid & Polymer Science*. 2004;282(11):1299-.
- [48] Freitag M, Martin Y, Misewich J, Martel R, Avouris P. Photoconductivity of single carbon nanotubes. *Nano Letters*. 2003;3(8):1067-71.
- [49] Martinez A, Fuse K, Xu B, Yamashita S. Optical deposition of graphene and carbon nanotubes in a fiber ferrule for passive mode-locked lasing. *Optics Express*. 2010;18(22):23054-61.
- [50] Kashiwagi K, Yamashita S, Set SY. In-situ monitoring of optical deposition of carbon nanotubes onto fiber end. *Opt Express*. 2009 03/30;17(7):5711-5.
- [51] Kashiwagi K, Yamashita S. Deposition of carbon nanotubes around microfiber via evanescent light. *Opt Express*. 2009 09/28;17(20):18364-70.
- [52] Nicholson J, Windeler R, DiGiovanni D. Optically driven deposition of single-walled carbon-nanotube saturable absorbers on optical fiber end-faces. *Optics Express*. 2007;15(15):9176-83.
- [53] Ji H, Oxenløwe LK, Galili M, Rottwitt K, Jeppesen P, Grüner-Nielsen L, editors. Fiber optical trap deposition of carbon nanotubes on fiber end-faces in a modelocked laser. *Conference on Lasers and Electro-Optics; 2008: Optical Society of America*.
- [54] Nicholson JW, editor *Optically assisted deposition of carbon nanotube saturable absorbers. Lasers and Electro-Optics, 2007 CLEO 2007 Conference on; 2007 6-11 May 2007*.
- [55] Lamhot Y, Barak A, Peleg O, Segev M. Self-trapping of optical beams through thermophoresis. *Physical review letters*. 2010;105(16):163906.
- [56] Ismail M, Ahmad F, Harun S, Arof H, Ahmad H. A Q-switched erbium-doped fiber laser with a graphene saturable absorber. *Laser Physics Letters*. 2013;10(2):025102.
- [57] Harun S, Ismail M, Ahmad F, Ismail M, Nor R, Zulkepely N, et al. A Q-switched erbium-doped fiber laser with a carbon nanotube based saturable absorber. *Chinese Physics Letters*. 2012;29(11):114202.
- [58] Harun SW, Ahmad H, Ismail MA, Ahmad F, editors. Q-switched and soliton pulses generation based on carbon nanotubes saturable absorber. *Electronics, Communications and Photonics Conference (SIEPC), 2013 Saudi International; 2013: IEEE*.
- [59] Martinez A, Fuse K, Yamashita S. Mechanical exfoliation of graphene for the passive mode-locking of fiber lasers. *Applied Physics Letters*. 2011 09/19;99(12):121107-3.
- [60] Chang YM, Kim H, Lee JH, Song YW. Multilayered graphene efficiently formed by mechanical exfoliation for nonlinear saturable absorbers in fiber mode-locked lasers. *Applied Physics Letters*. 2010;97(21):211102--3.

- [61] Yang Y, Chow K, editors. Optical pulse generation using multi-layered graphene saturable absorber. Information, Communications and Signal Processing (ICICS) 2013 9th International Conference on; 2013: IEEE.
- [62] Chang YM, Kim H, Lee JH, Song Y-W, editors. Passive mode-locker incorporating physically exfoliated graphene for fiber ring lasers. Optical Fiber Communication Conference; 2011: Optical Society of America.
- [63] Saidin N, Zen DIM, Ahmad F, Damanhuri SSA, Ahmad H, Dimiyati K, et al. Q-switched thulium-doped fibre laser operating at 1900 nm using multi-layered graphene based saturable absorber. *Iet Optoelectronics*. 2014;8(4):155-60.
- [64] Yamashita S, Set SY, Goh CS, Kikuchi K. Ultrafast saturable absorbers based on carbon nanotubes and their applications to passively mode-locked fiber lasers. *Electronics and Communications in Japan (Part II: Electronics)*. 2007;90(2):17-24.
- [65] Yamashita S, Inoue Y, Maruyama S, Murakami Y, Yaguchi H, Jablonski M, et al. Saturable absorbers incorporating carbon nanotubes directly synthesized onto substrates and fibers and their application to mode-locked fiber lasers. *Optics letters*. 2004;29(14):1581-3.
- [66] Wang F, Torrisi F, Jiang Z, Popa D, Hasan T, Sun Z, et al., editors. Graphene passively Q-switched two-micron fiber lasers. *CLEO: Science and Innovations*; 2012: Optical Society of America.
- [67] Popa D, Sun Z, Torrisi F, Hasan T, Wang F, Ferrari A. Sub 200 fs pulse generation from a graphene mode-locked fiber laser. *Applied Physics Letters*. 2010;97(20):203106.
- [68] Hasan T, Sun Z, Wang F, Bonaccorso F, Tan PH, Rozhin AG, et al. Nanotube-polymer composites for ultrafast photonics. *Advanced materials*. 2009;21(38-39):3874-99.
- [69] Kelleher E, Travers J, Sun Z, Rozhin A, Ferrari A, Popov S, et al. Nanosecond-pulse fiber lasers mode-locked with nanotubes. *Applied Physics Letters*. 2009;95(11):111108--3.
- [70] Wang J, Luo Z, Zhou M, Ye C, Fu H, Cai Z, et al. Evanescent-light deposition of graphene onto tapered fibers for passive Q-switch and mode-locker. *Photonics Journal, IEEE*. 2012;4(5):1295-305.
- [71] Song Y-W, Yamashita S, Goh CS, Set SY. Carbon nanotube mode lockers with enhanced nonlinearity via evanescent field interaction in D-shaped fibers. *Opt Lett*. 2007 01/15;32(2):148-50.
- [72] Lin Y-H, Yang C-Y, Liou J-H, Yu C-P, Lin G-R. Using graphene nano-particle embedded in photonic crystal fiber for evanescent wave mode-locking of fiber laser. *Optics Express*. 2013 2013/07/15;21(14):16763-76.

- [73] Zhao J, Ruan S, Yan P, Zhang H, Yu Y, Wei H, et al. Cladding-filled graphene in a photonic crystal fiber as a saturable absorber and its first application for ultrafast all-fiber laser. *Optical Engineering*. 2013;52(10):106105-.
- [74] Digonnet MJF. *Rare-Earth-Doped Fiber Lasers and Amplifiers, Revised and Expanded*: CRC; 2001.
- [75] Zayhowski JJ, Dill III C. Diode-pumped passively Q-switched picosecond microchip lasers. *Opt Lett*. 1994 09/15;19(18):1427-9.
- [76] Zayhowski JJ, Kelley PL. Optimization of Q-switched lasers. *Quantum Electronics, IEEE Journal of*. 1991;27(9):2220-5.
- [77] Novoselov K, Geim A, Morozov S, Jiang D, Zhang Y, Dubonos S, et al. Electric field effect in atomically thin carbon films. *Science*. 2004;306(5696):666-9.
- [78] Spühler G, Paschotta R, Fluck R, Braun B, Moser M, Zhang G, et al. Experimentally confirmed design guidelines for passively Q-switched microchip lasers using semiconductor saturable absorbers. *JOSA B*. 1999;16(3):376-88.
- [79] Yang D, Velamakanni A, Bozoklu G, Park S, Stoller M, Piner RD, et al. Chemical analysis of graphene oxide films after heat and chemical treatments by X-ray photoelectron and micro-Raman spectroscopy. *Carbon*. 2009;47(1):145-52.
- [80] Zhu Y, Murali S, Cai W, Li X, Suk JW, Potts JR, et al. Graphene and graphene oxide: synthesis, properties, and applications. *Advanced materials*. 2010;22(35):3906-24.
- [81] Graphene Laboratories Inc. Available from: <https://graphene-supermarket.com/>.

